14. Outbursting Young Stellar Object PGIR 20dci in the Perseus Arm
Lynne A. Hillenbrand, et al.

15. The Pictoris b Hill sphere transit campaign. Paper I: Photometric limits to dust and rings
M. A. Kenworthy, et al.

16. The warm-up phase in massive star-forming cores around RCW 120
M. S. Kirsanova, et al.

17. New low-mass members of Chamaeleon I and Cha
K. Kubiak, et al.

18. ALMA Observations of Massive Clouds in the Central Molecular Zone: Ubiquitous Protostellar Outflows
Xing Lu, et al.

19. Characterizing the dust content of disk substructures in TW Hya
Enrique Macias, et al.

20. Radiative scale-height and shadows in protoplanetary disks
Matías Montesinos, et al.

14. Outbursting Young Stellar Object PGIR 20dci in the Perseus Arm
Lynne A. Hillenbrand, et al.

We report the discovery of a likely outbursting Class I young stellar object, associated with the star-forming region NGC 281-W (distance $\sim$ 2.8 kpc). The source is currently seen only at infrared wavelengths, appearing in both the Palomar Gattini InfraRed (1.2 μm) and the Near Earth Object Widefield Infrared Survey Explorer (3.4 and 4.6 μm) photometric time-domain surveys. Recent near-infrared imaging reveals a new, extended scattered light nebula. Recent near-infrared spectroscopy confirms the similarity of PGIR 20dci to FU Ori type sources, based on strong molecular absorption in CO, H_2O, and OH, weak absorption in several atomic lines, and a warm wind/outflow as indicated by a P Cygni profile in the He I 10830 Å line. This is a rare case of an FU Ori star with a well-measured long term photometric rise before a sharper outburst, and the second instance of an FU Ori star with a documented two-step brightening in the mid-infrared.

15. The Pictoris b Hill sphere transit campaign. Paper I: Photometric limits to dust ar

M. A. Kenworthy, et al.

Aims. Photometric monitoring of β Pic in 1981 showed anomalous fluctuations of up to 4% over several days, consistent with foreground material transiting the stellar disk. The subsequent discovery of the gas giant planet β Pic b and the predicted transit of its Hill sphere to within 0.1 au of the planet provided an opportunity to search for the transit of a circumplanetary disk (CPD) in this 21 ± 4 Myr-old planetary system. We aim to detect or put an upper limit of the density and nature of the material in the circumplanetary environment of the planet through continuous photometric monitoring of the Hill sphere transit in 2017 and 2018.

Methods. Continuous broadband photometric monitoring of β Pic requires ground-based observatories at multiple longitudes to provide redundancy and to provide triggers for rapid spectroscopic followup. These observatories include the dedicated β Pic monitoring observatory bRing at Sutherland and Siding Springs, the ASTEP400 telescope at Concordia, and observations from the space observatories BRITE and Hubble Space Telescope (*HST*). We search the combined light curves for evidence of short period transient events caused by rings and for longer term photometric variability due to diffuse circumplanetary material.

Results. We find no photometric event that matches with the event seen in November 1981, and there is no systematic photometric dimming of the star as a function of the Hill sphere radius.

Conclusions. We conclude that the 1981 event was not caused by the transit of a CPD around β Pic b. The upper limit on the long term variability of β Pic places an upper limit of 1.8×10^{22} g of dust within the Hill sphere (comparable to the ~100 km-radius asteroid 16 Psyche). Circumplanetary material is either condensed into a disk that does not transit β Pic, is condensed into a disk with moons that has an obliquity that does not intersect with the path of β Pic behind the Hill sphere, or is below our detection threshold. This is the first time that a dedicated international campaign has mapped the Hill sphere transit of a gas giant extrasolar planet at 10 au.

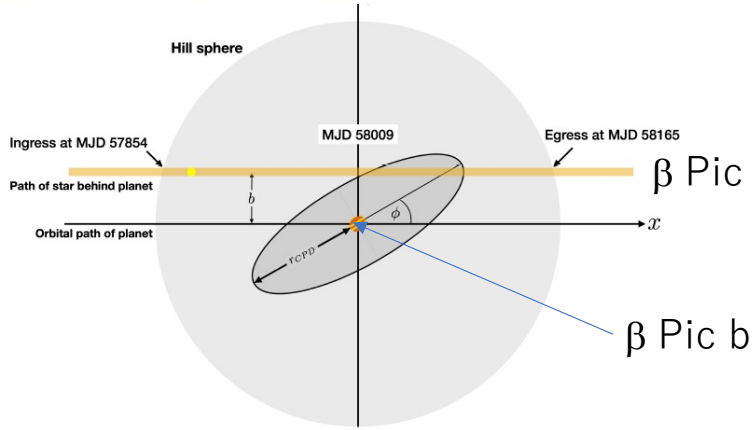

β Pic　M=1.797$M_\odot$, τ=21Myr
β Pic b m=11.1M_J, a=9.76AU
r_{Hill} =1.1AU

1981 β Pic 4% 数日明るさの変動
β　Pic b の周惑星円盤による掩蔽？
2017,2018 β Pic の光度モニター

予想時期に暗くなった形成はなし。

16. The warm-up phase in massive star-forming cores around RCW 120
M. S. Kirsanova, et al.

We study molecular emission in a massive condensation at the border of the H II region RCW 120, paying particular attention to the Core 1 and Core 2 objects, the most massive fragments of the condensation found previously by ALMA. The latter fragment was previously suggested to host a high-mass analogue of Class 0 young stellar object. We present spectra of molecular emission in the 1 mm range made with the APEX telescope. We detect CH_3OH and $C^{34}S$ lines in Core 1 and Core 2. The CH_3CN series and the SO_2 lines are only found in Core 2. We estimate gas physical parameters using methanol lines and obtain gas temperature less than 100 K in both regions. Molecular hydrogen number density in Core 2 is in the range of $10^5 - 10^7$ cm^{-3} and is more uncertain in Core 1. However, the detection of the CH_3CN lines corresponding to highly excited transitions (E_u > 400 K) in Core 2 indicates that the region contains hot gas, while the abundances of CH_3OH, CS, SO_2 and CH_3CN are quite low for a hot core stage. We propose that Core 2 is in the warm-up phase prior to the establishing of the hot gas chemistry. We suggest that Core 2 is in the beginning of the hot core stage. There are no detected CH_3CN lines in Core 1, therefore, it might be on an even less evolved evolutionary stage.

Herschel image 70 μm

ATLASGAL 870 μm

コア1

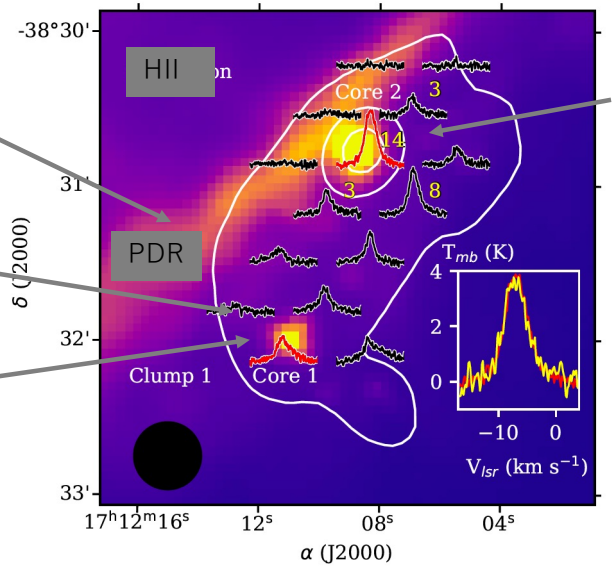

コア2

コア1	コア2
CH3OH, C34S	CH3OH, C34S CH3CN, SO2
T<100K	K<100K
	n~$10^{5\text{-}7}$cm^{-3}
Less evolved	分子少ない。 Warm-up phase

17. New low-mass members of Chamaeleon I and ε Cha

K. Kubiak, et al.

Aims. The goal of this paper is to increase the membership list of the Chamaeleon star forming region and the ϵ Cha moving group, in particular for low-mass stars and substellar objects. We extended the search region significantly beyond the dark clouds.
Methods. Our sample has been selected based on proper motions and colours obtained from *Gaia* and 2MASS. We present and discuss the optical spectroscopic follow-up of 18 low-mass stellar objects in Cha I and ϵ Cha. We characterize the properties of objects by deriving their physical parameters, both from spectroscopy and photometry.
Results. We add three more low-mass members to the list of Cha I, and increase the census of known ϵ Cha members by more than 40%, confirming spectroscopically 13 new members and relying on X-ray emission as youth indicator for 2 more. In most cases the best-fitting spectral template is from objects in the TW Hya association, indicating that ϵ Cha has a similar age. The first estimate of the slope of the initial mass function in ϵ Cha down to the sub-stellar regime is consistent with that of other young clusters. We estimate our IMF to be complete down to ≈ 0.03 $M_\odot$. The IMF can be represented by two power laws: for $M < 0.5$ $M_\odot$ $\alpha = 0.42 \pm 0.11$ and for $M > 0.5$ $M_\odot$ $\alpha = 1.44 \pm 0.12$.
Conclusions. We find similarities between ϵ Cha and the southernmost part of Lower Centaurus Crux (LCC A0), both lying at similar distances and sharing the same proper motions. This suggests that ϵ Cha and LCC A0 may have been born during the same star formation event

カメレオン領域の星形成史
Cha I D=190pc 250YSOs (~2Myr)
Cha II D=210pc 51YSOs (2-4Myr)
Cha III No YSOs
ε Cha moving group (5-10 Myr)

Gaia + 2 MASS

Hα emission line EW, a shallow Na I absorption,
mid IR excess, X-ray ➔ pre-main-sequence

Cha I 7個、Cha II 2個、ε Cha 15個

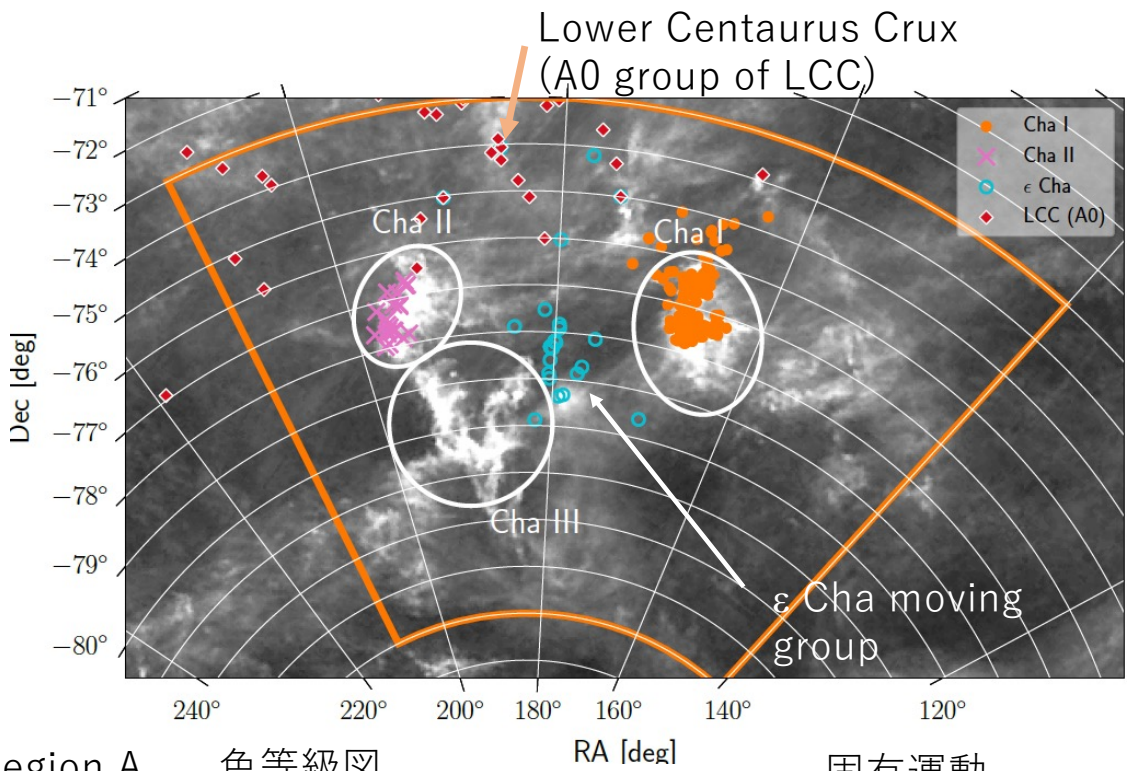

3D構造

2MASSJバンドソースの距離別分布

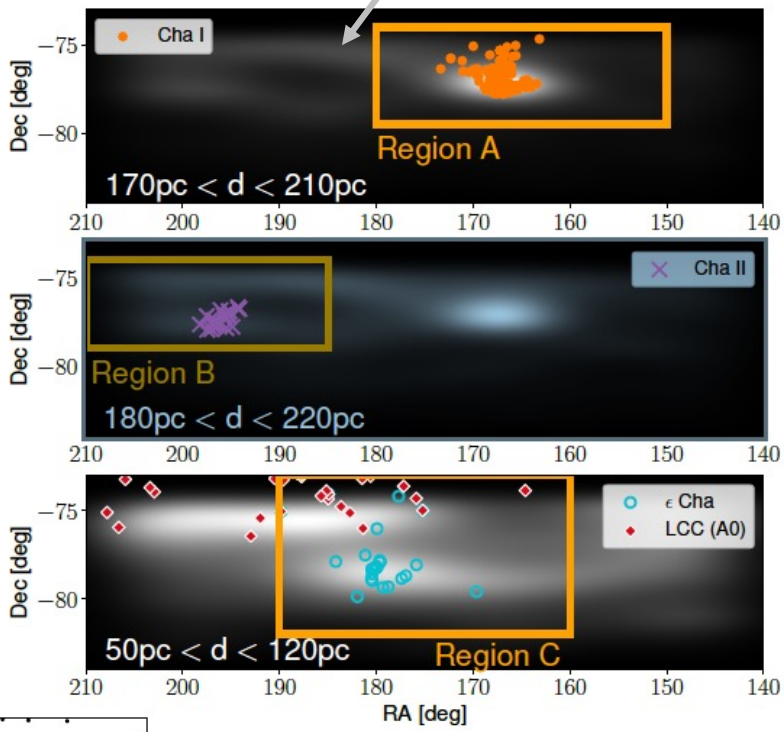

Region A　色等級図

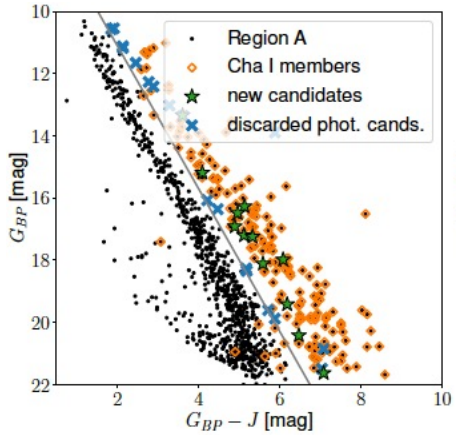

固有運動

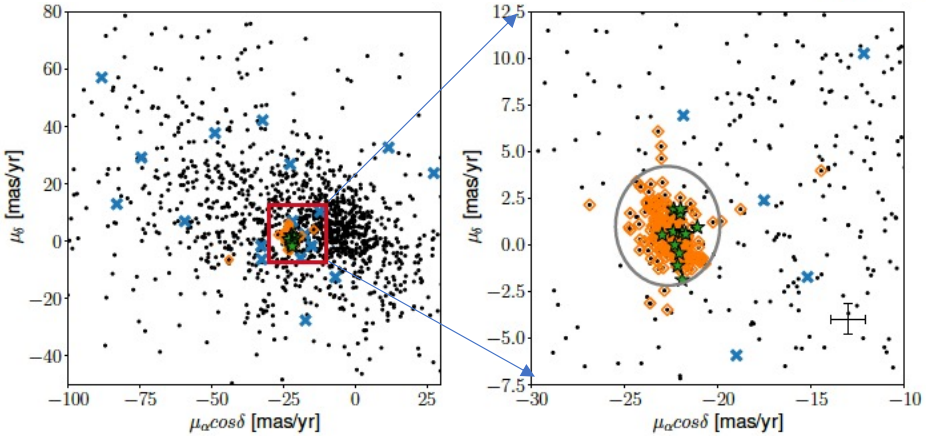

分光：ε Chaの年齢 8-10 Myr

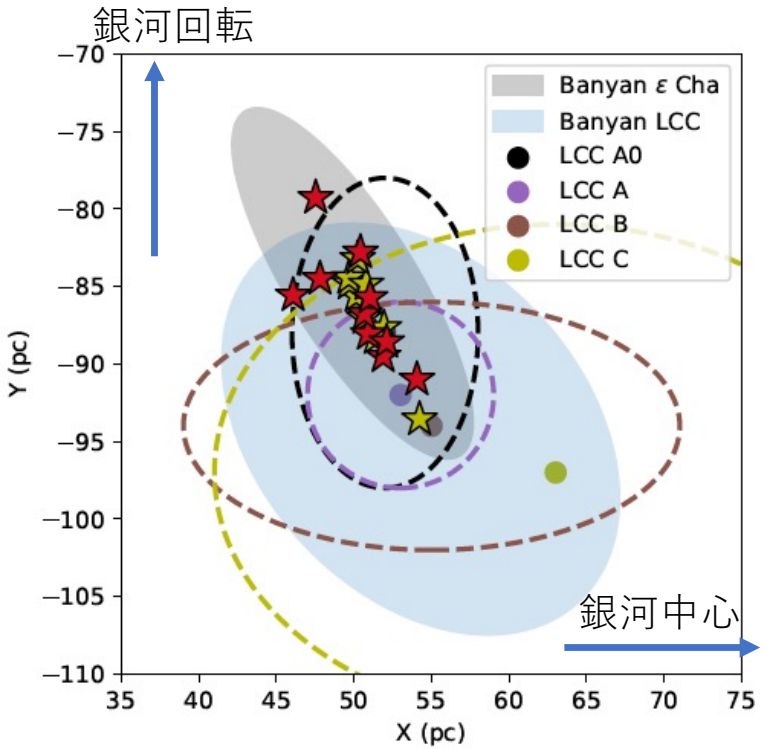

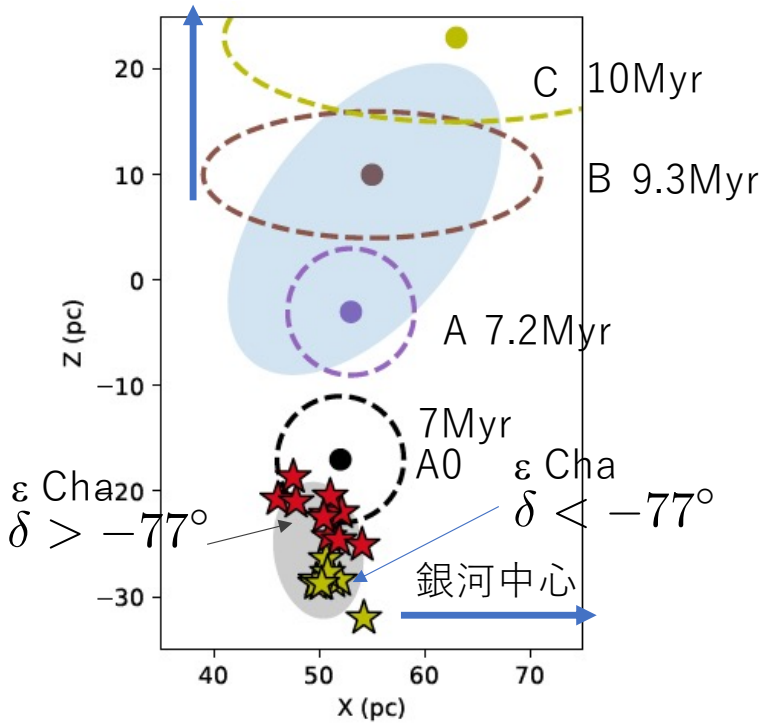

LCC from Goodman+2018

18. ALMA Observations of Massive Clouds in the Central Molecular Zone: Ubiquitous Protostellar Outflows
Xing Lu, et al.

We observe 1.3 mm spectral lines at 2000 AU resolution toward four massive molecular clouds in the Central Molecular Zone of the Galaxy to investigate their star formation activities. We focus on several potential shock tracers that are usually abundant in protostellar outflows, including SiO, SO, CH_3OH, H_2CO, HC_3N, and HNCO. We identify 43 protostellar outflows, including 37 highly likely ones and 6 candidates. The outflows are found toward both known high-mass star forming cores and less massive, seemingly quiescent cores, while 791 out of the 834 cores identified based on the continuum do not have detected outflows. The outflow masses range from less than 1 $M_\odot$ to a few tens of $M_\odot$, with typical uncertainties of a factor of 70. We do not find evidence of disagreement between relative molecular abundances in these outflows and in nearby analogs such as the well-studied L1157 and NGC7538S outflows. The results suggest that i) protostellar accretion disks driving outflows ubiquitously exist in the CMZ environment, ii) the large fraction of candidate starless cores is expected if these clouds are at very early evolutionary phases, with a caveat on the potential incompleteness of the outflows, iii) high-mass and low-mass star formation is ongoing simultaneously in these clouds, and iv) current data do not show evidence of difference between the shock chemistry in the outflows that determines the molecular abundances in the CMZ environment and in nearby clouds.

CMZは、星形成効率が10倍くらい低い。
Lu+2020 ALMA conti → 2000AU規模、834個のコア →
ここで、skockトレーサーでアウトフローは見つかるか。

37(highly likely)+6(candidate)
791 no detection

H2Oメーザー源　　1.3mm 連続波

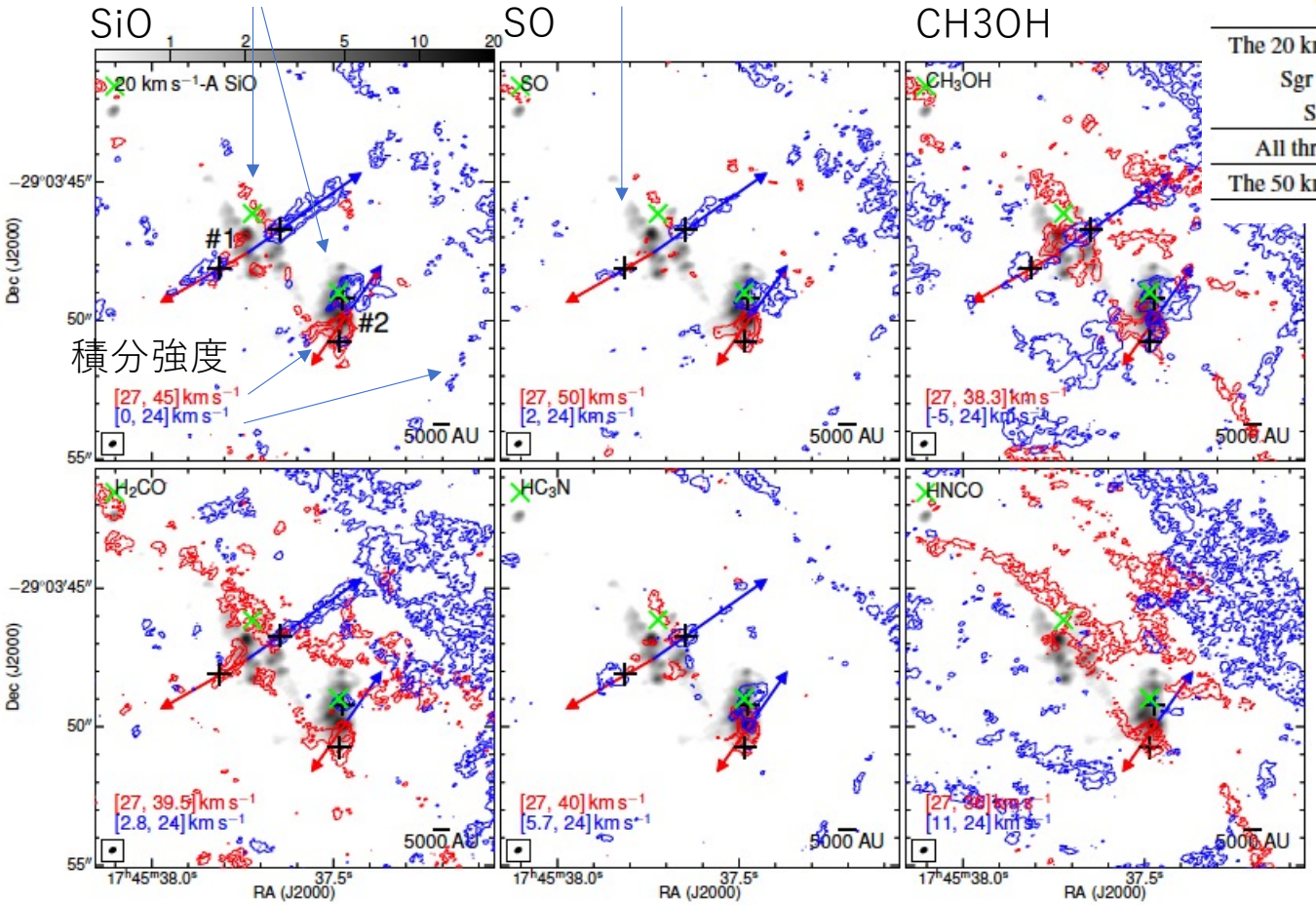

τ ~10Myr(ℓ /1度)
Vorb~80km/s

Longmore+2013

Cloud	V_{lsr}	No. of cores	No. of outflows	Fraction with outflows
(1)	(2)	(3)	(4)	(5)
The 20 km s^{-1} cloud	12.5	471	20	0.042
Sgr B1-off	31.1	89	5	0.056
Sgr C	−52.6	274	18	0.066
All three clouds	...	834	43	0.052
The 50 km s^{-1} cloud	48.6	0	0	...

834コア
43コアがアウトフロー付き
残り791コアがなし。
★分子雲により
4~7%がアウトフロー付き

τ prestellar期
=1-2Myrなら
τ outflow付き
=0.05-0.1Myr

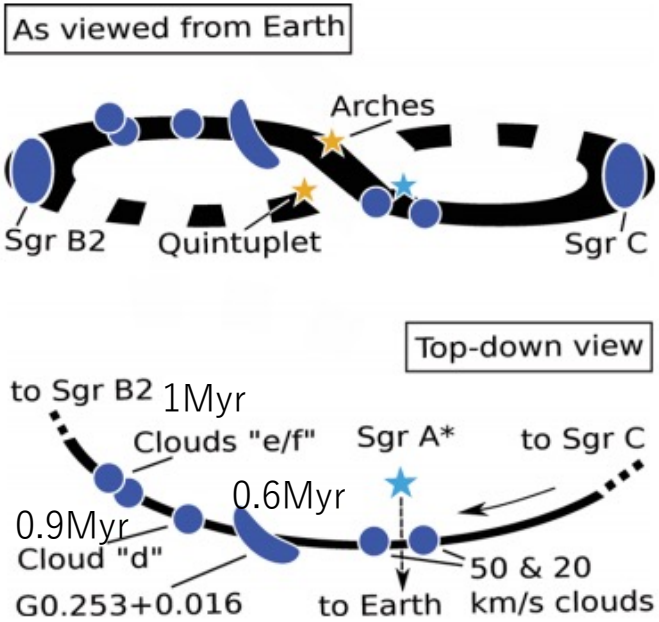

H2に相対的なabundance

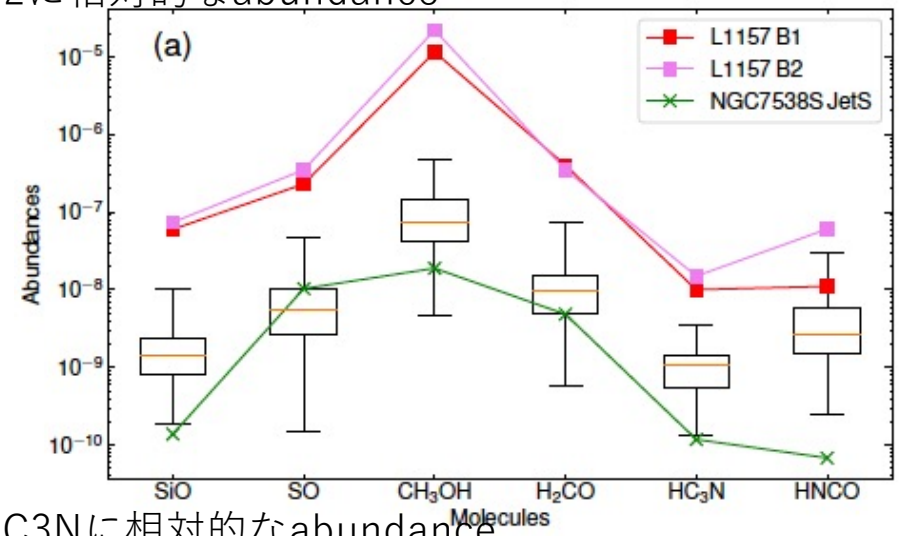

HC3Nに相対的なabundance

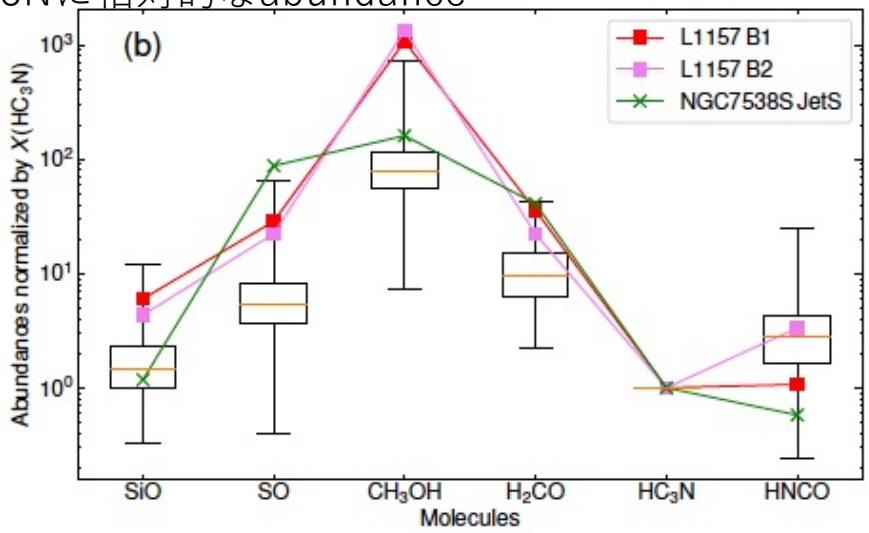

L1157 low mass star formation
NGC 7538 S high mass star formation

L1157でCOが光学的に厚くなっている可能性
(Bachiller & Pérez Gutiérrez 1997)
H2を過小評価。
shock tracer 分子の存在比を過大評価

HC3Nに相対的な存在比

CMZの特殊性は見られない。

19. Characterizing the dust content of disk substructures in TW Hya
Enrique Macias, et al.

Context. A key piece of information to understand the origin and role of protoplanetary disk substructures is their dust content. In particular, disk substructures associated with gas pressure bumps can work as dust traps, accumulating grains and reaching the necessary conditions to trigger the streaming instability.
Aims. In order to shed some light on the origin and role that disk substructures play in planet formation, we aim at characterizing the dust content of substructures in the disk of TW Hya.
Methods. We present Atacama Large Millimeter Array (ALMA) observations of TW Hya at 3.1 mm with $\sim$ 50 milliarcsecond resolution. These new data were combined with archival high angular resolution ALMA observations at 0.87 mm, 1.3 mm, and 2.1 mm. We analyze these multi-wavelength data to infer a disk radial profile of the dust surface density, maximum particle size, and slope of the particle size distribution.
Results. Most previously known annular substructures in the disk of TW Hya are resolved at the four wavelengths. Inside the inner 3 au cavity, the 2.1 mm and 3.1 mm images show a compact source of free-free emission, likely associated with an ionized jet. Our multi-wavelength analysis of the dust emission shows that the maximum particle size in the disk of TW Hya is $>$ 1 mm. The inner 20 au are completely optically thick at all four bands, which results in the data tracing different disk heights at different wavelengths. Coupled with the effects of dust settling, this prevents the derivation of accurate density and grain size estimates in these regions. At $r > 20$ au, we find evidence of the accumulation of large dust particle at the position of the bright rings, indicating that these are working as dust traps. The total dust mass in the disk is between 250 and 330 $M_{\oplus}$, which represents a gas-to-dust mass ratio between 50 and 70. Our mass measurement is a factor of 4.5-5.9 higher than the mass that one would estimate using the typical assumptions of large demographic surveys.
Conclusions. Our results indicate that the ring substructures in TW Hya are ideal locations to trigger the streaming instability and form new generations of planetesimals.

20. Radiative scale-height and shadows in protoplanetary disks
Matías Montesinos, et al.

Planets form in young circumstellar disks called protoplanetary disks. However, it is still difficult to catch planet formation in-situ. Nevertheless, from recent ALMA/SPHERE data, encouraging evidence of the direct and indirect presence of embedded planets has been identified in disks around young stars: co-moving point sources, gravitational perturbations, rings, cavities, and emission dips or shadows cast on disks.

The interpretation of these observations needs a robust physical framework to deduce the complex disk geometry. In particular, protoplanetary disk models usually assume the gas pressure scale-height given by the ratio of the sound speed over the azimuthal velocity $H/r = c_s/v_k$. By doing so, *radiative* pressure fields are often ignored, which could lead to a misinterpretation of the real vertical structure of such disks.

We follow the evolution of a gaseous disk with an embedded Jupiter mass planet through hydrodynamical simulations, computing the disk scale-height including radiative pressure, which was derived from a generalization of the stellar atmosphere theory. We focus on the vertical impact of the radiative pressure in the vicinity of circumplanetary disks, where temperatures can reach $\gtrsim$ 1000 K for an accreting planet, and radiative forces can overcome gravitational forces from the planet.

The radiation-pressure effects create a vertical optically thick column of gas and dust at the proto-planet location, casting a shadow in scattered light. This mechanism could explain the peculiar illumination patterns observed in some disks around young stars such as HD 169142 where a moving shadow has been detected, or the extremely high aspect-ratio $H/r \sim 0.2$ observed in systems like AB Aur and CT Cha.

$$\frac{dP}{dz} = -\int \rho \nabla \Psi dz, \qquad (1)$$

$$\frac{1}{\rho}\frac{\partial P}{\partial z} = -\frac{GM_*}{(r^2+z^2)^{(3/2)}} - \frac{GM_p}{(s^2+z^2)^{(3/2)}}, \qquad (2)$$

$$P = \int p \, dz,$$

$$\Sigma \frac{d\boldsymbol{u}}{dt} = -\nabla P - \int \rho \nabla \Psi \, dz,$$

$$\frac{1}{\rho}\frac{\partial p}{\partial z} = -\frac{GM_* z}{(r^2+z^2)^{\frac{3}{2}}} \approx -\frac{GM_* z}{r^3} \equiv -\Omega_K^2 z.$$

Muller, Kley, Meru 2012